A COMPARISON OF SPECTRAL MIXTURE ANALYSIS METHODS FOR URBAN LANDSCAPE USING LANDSAT ETM+ DATA: LOS ANGELES, CA

Xianfeng Chen [a] and Lin Li [b]

[a] Slippery Rock University of Pennsylvania, Slippery Rock, PA 16507, USA – xianfeng.chen@sru.edu
[b] Indiana University-Purdue University, Indianapolis, IN 46202, USA – ll3@iupui.edu

ABSTRACT：

Although spectral mixture analysis has been widely used for mapping the abundances of physical components of urban surface with moderate spatial resolution satellite imagery recently, the spectral heterogeneity of urban land surface has still posed a great challenge to accurately estimate fractions of surface materials within a pixel. How to dealing with the highly spectral heterogeneous nature of urban land surface remains a scientific question. In this study, a comparison of different spectral mixture models was carried out to examine the performance of each model in dealing with spectral variability of urban surface. The comparison is focused on spectral normalized models and multiple endmember spectral mixture analysis (MESMA). Two spectral normalization algorithms, mean normalization and hyperspheric direction cosine (HSDC) normalization, were applied to Landsat ETM+ data acquired over Los Angeles, CA. A total of 170 spectral mixture models of two, three, and four endmembers were employed with MESMA. The reference data digitized from Arc2Earth was used to evaluated the mapping results. The results showed that MESMA is a promising tool to map abundances of urban surface components. Relative high mapping accuracies were achieved for vegetations and impervious surfaces. R2 and Root mean square error (RMSE) of vegetation fraction are 0.79 and 7.1%, respectively. The estimation of impervious surfaces obtained similar accuracy, with R2 0.72 and RMSE 10.7%. Both mean and HSDC normalized models made a notable improvement in mapping vegetation fraction and slight improvement in mapping impervious surface fractions, comparing with the standard SMA. Both two normalizations can only suppress spectral variation with similar spectral shape. HSDC is slightly better than mean normalization in reducing the effects of illumination and spectral variability of urban land surface.

1. INTRODUCTION

With the rapid population growth, urbanization has become a common trend all over the world since the 20th century. Urban land use and land cover (LULC) change has caused major concerns due to relevant environmental issues such as deforestation, air and water pollution, and urban heat islands. Therefore, monitoring the dynamic change of urban LULC has been imperative for understanding and managing urban environment, and remote sensing can provide effective means for such efforts. Moderate spatial resolution multispectral satellite remotely sensed data (e.g. Landsat MSS, TM, and ETM, SPOT HRV and HRVIR), in particular, have been widely used for this purpose due to their worldwide availability.

A variety of algorithms have been applied to extract feature and property information of urban land surfaces, including the conventional statistic-based, neural network, rule-based, and object-based methods. However, the presence of spectrally mixed pixels has been a consistent challenge facing pixel-based approaches since mixed pixels tend to be misclassified. For instance, a 30-m pixel in residential areas may contain lawn, roof, and drive way elements at the same time. Spectral mixture analysis (SMA), based on a physical mixture model, has ability to extract sub-pixel information such as the abundances of each endmember presented in the pixel (Adams, 1986; Adams et al., 1993). For LULC types, the SMA models can be regarded as a linear combination of fractions of all endmembers (Adams et al., 1995; Robert, et al., 1998). Numerous studies have demonstrated that linear spectral mixture analysis (LSMA) is a promising technique for the extraction of fractions of LULC types (Adams et al., 1995; Small, 2001, 2003, 2004; Wu and Murray, 2003; Wu, 2004; Powell et al., 2007). Small (2001)

estimated urban vegetation abundance based on a LSMA with three endmembers, vegetation, high albedo, and low albedo surfaces. Wu and Murray (2003) focused on computing urban impervious surface using a conceptual model: vegetation, impervious surface, and soil component (VIS see Ridd, 1995). The high spectral variability of urban surface materials impedes the efforts of accurately extracting the abundances of land cover components (Small 2005). To suppress spectral variability of impervious surfaces, Wu (2004) first normalized pixel reflectance of each band with mean reflectance, and then applied LSMA to a normalized image. An alternative approach to address the high spectral heterogeneity of urban surface is the multiple end member spectral mixture analysis (MESMA see Roberts et al., 1998). Compared to traditional LSMA using a fixed number of endmembers for the entire scene, MESMA allows the number and types of endmembers to vary from pixel to pixel. Rashed et al. (2003) and Powell et al. (2007) demonstrated the potential of using MESMA to extract the abundances of urban surface components.

The above studies have gained success to a certain degree in estimating abundances of urban surface materials. However, different approaches vary in dealing with spectral variation of urban surface types. There are two questions remaining unaddressed. First, how well does normalized LSMA reduce the effects of spectral variability and shade? Second, which approach has the best performance of handling spectral variability? In this study, several LSMA algorithms applied to Landsat ETM+ data of Los Angles, CA were examined for extracting the information of abundance of urban surface types: high albedo, low albedo, soil, and vegetation. These algorithms include standard LSMA, normalized LSMA, and MESMA. Two algorithms, normalized with mean reflectance (Wu, 2004)

and hyperspherical direction cosine transformation (HSDC: see Pouch and Campagna, 1990) were used for reflectance normalization.

2. STUAY SITE

The study site (Figure 1) is located in Los Angeles, CA. There are over eight million people in Los Angeles, the second largest city in the United States. Los Angeles is also famous with the most diverse culture in USA. The climate in Los Angeles belongs to a typical Mediterranean climate with hot, dry summer and wet, cool winter. The natural vegetation includes grass, scrub, and chaparral. The study area includes Western Hollywood, South Pasadena, and Downtown Los Angeles. A wide variety of urban land use and land cover types present in the study area. It is an ideal test site for urban landscape analysis.

3. DATA AND METHODS

3.1 Data

Landsat ETM+ data was acquired over the study site on May 1, 2000, under a cloud free weather condition. A black and white digital orthphoto quadrant (DOQQ) with 1-meter spatial resolution acquired in 1996 was
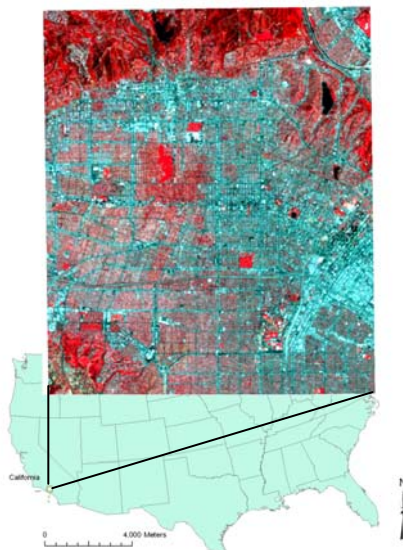

Figure 1. Study site of Los Angeles (Landsat ETM+ false Color composite)

used for image rectification. A 1-foot spatial resolution true color aerial imagery data from Arc2Earth, a new product that allows users to visualize spatial data from Google Earth within ESRI's ArcGIS, was used for extraction of reference data. The true color aerial imagery was acquired in 2004.

3.2 Data preprocessing

The image rectification, conversion of digital number to radiance, and the conversion of radiance to surface reflectance, were performed to ETM+ data. 96 ground control points from the whole scene were collected for image rectification. A second order of polynomial transformation was applied to ETM+ data resulting the root mean square error around 20

meter. The digital numbers of image pixels were converted to radiance following a routine procedure proposed by Markham et al. (1997). A reflectance retrieval algorithm modified from the routine procedure developed by Markham et al. (1997) was used to retrieve surface reflectance in which the atmospheric effect was taken into consideration (Chuvieco et al. 2002). For atmospheric correction, the atmospheric path radiance was estimated from dark object (deep water) whereas the atmospheric transimissivity was simply regarded as function of the cosine of the zenith angle (Chavez, 1996).

3.3 Endmember collection

For all LSMA, endmembers were selected following the routine procedures: 1) minimum noise fraction (MNF) transformation (Green et al., 1988) was
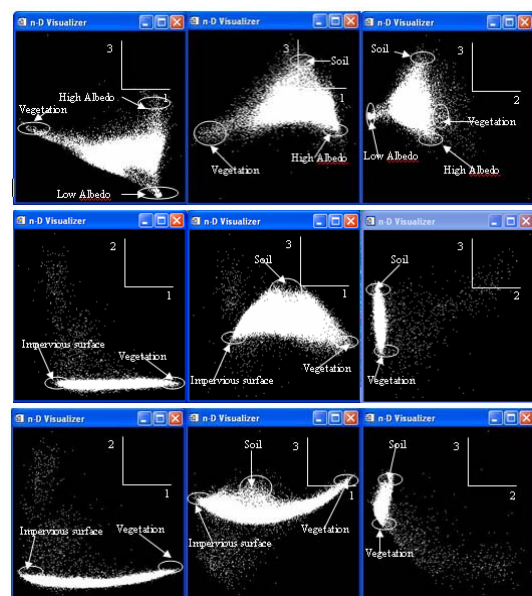

Figure 2. Scatter plots of three MNF components upper: regular ETM+ data; middle: mean normalized data; lower: HSDC normalized data

applied to ETM+ reflectance data in order to reduce data dimensionality and suppress the noise in the data; 2) pixel purity index (PPI, see Boardman et al., 1995) was calculate; 3) the relative pure pixels whose PPI are greater than threshold defined by users were plotted on n-dimensional feature spaces and the extreme pixels on scatter plot were selected as endmembers. For standard LSMA, four endmembers such as high albedo surface, low albedo surface, vegetation, and soil, were chosen (Figure 2). There were only three endmembers chosen for normalized LSMA – impervious surface, vegetation, and soil. The endmember selection of MESMA was based on the results of standard LSMA. Pixels with high residue were checked using Arc2Earth with assumption that inappropriate endmembers may result in high residues. There were a total of nine endmembers collected for MESMA, including white roof, red roof, concrete surface, asphalt surface, fresh asphalt surface, grass, wood, soil, and deep shade/water.

3.4 SMA Models

3.3.1   Standard LSMA   The standard LSMA is expressed as Equation 1 in which the reflectance of each pixel

can be decomposed into linear composition of endmembers weighed with their fractions and the residue assuming multiple back scatter effects are negligible (Adams, 1986; Adams et al., 1993).

$$R_\lambda = \sum_{i=1}^{N} f_i R_{i,\lambda} + e_\lambda \qquad (1)$$

Where R_λ = the reflectance at band λ
f_i = the fraction of endmember i
$R_{i\lambda}$ = the reflectance of endmember i at λ
N = the number of endmembers
e_λ = the residue at λ.

3.3.2 MESMA MESMA is a specific type of LSMA. Unlike standard LSMA, MESMA applies different sets of endmembers to LSMA model instead of a complete set of endmembers (Roberts et al., 1998). MESMA models vary from pixel to pixel. In this study, there were total 170 two-endmembers, three-endmembers, and four-endmembers models applied. The best model was determined based on its RMSE.

3.5 Spectral normalization

3.3.2 Mean normalization Mean normalization is proposed by Wu (2004) to reduce the effects of spectral variation for LSMA. It is expressed as following equation 2 and 3:

$$\mu = \frac{1}{N} \sum_{i=1}^{N} R_i \qquad (2)$$

$$\overline{R}_i = \frac{R_i}{\mu} \qquad (3)$$

Where m = the mean of reflectance in all bands
R_i = reflectance at band i
N = the number of bands
$\overline{R}i$ = normalized reflectance at band i

3.3.2 HSDC normalization HSDC is developed by Pouch and Campagna (1996) to suppress illumination effects and albedo variations. It is assumed that the radiance of pixel contains two components: illumination/albedo and spectral.

$$R = \sqrt{\sum_{i=1}^{N} R_i^2} \qquad (4)$$

$$\overline{R}_i = \frac{R_i}{R} \qquad (5)$$

Where R = illumination/albedo component

R_i = reflectance at band i
N = the number of bands
$\overline{R}i$ = normalized reflectance at band i

The illumination/albedo component is calculated based on equation 4. Equation 5 was used to normalize the reflectance at each band.

3.6 Models assessment

The model accuracies were assessed by referring to ground samples. 120 samples were selected randomly from the entire study area. Each sample covers 150×150 meter of surface in order to reduce the effects of geometric error, which is about 20 meter. The reference data of each sample were collected from 1-foot spatial resolution natural color aerial image using Arc2Earth. Four surface types such as high albedo, vegetation, soil, low albedo surface were digitized using ESRI's ArcGIS. Each category of urban land surface was summarized through ArcGIS geodatabase. The model predicted surfaces of each sample were compared with the reference information through a correlation analysis.
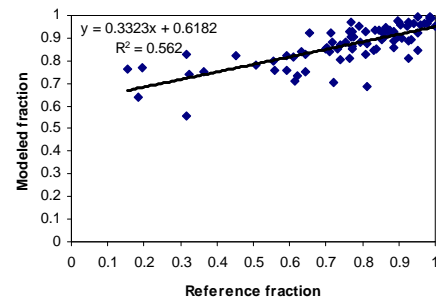

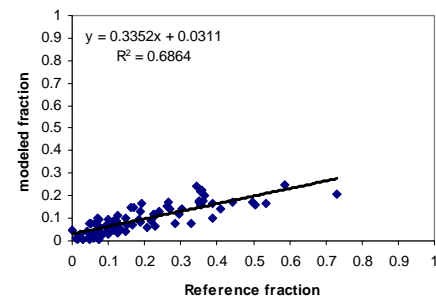Figure 3. Impervious surface scatter plot of LSMA

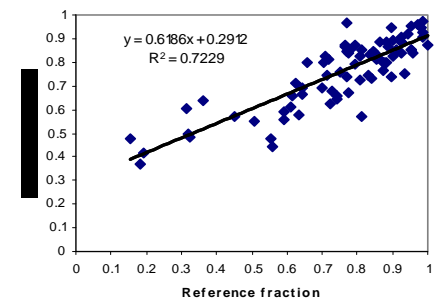

Figure 4. Vegetation scatter plot of LSMA

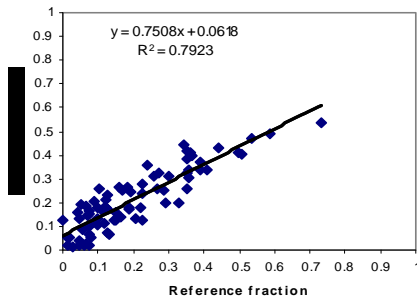Figure 5. Impervious surface scatter plot of MESMA

Figure 6. Vegetation scatter plot of LSMA
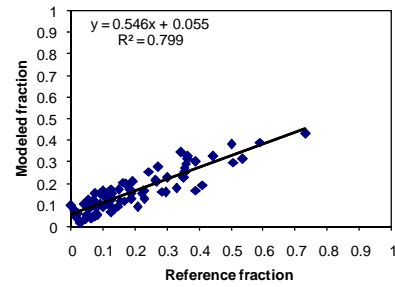

Figure 10. vegetation scatter plot of Mean normalized LSMA
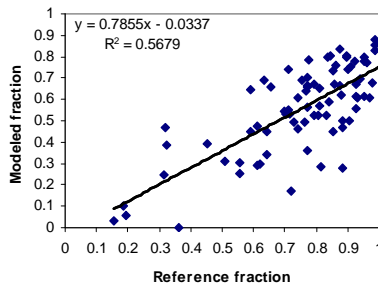

Figure 7. Impervious surface scatter plot of Mean normalized LSMA
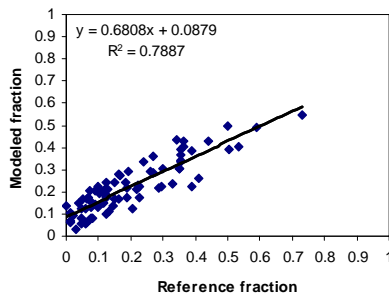

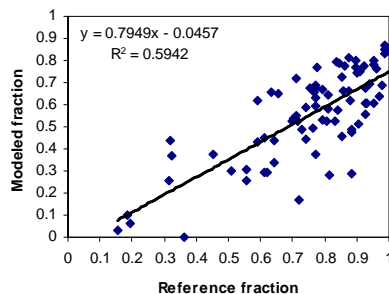Figure 8. Vegetation scatter plot of Mean normalized LSMA

Figure 9. Impervious surface scatter plot of Mean normalized LSMA

4. RESULTS AND CONCLUSIONS

The results of assessment showed that MESMA achieved the highest overall accuracy among all methods. It is not surprising that the spectral variations in high and low albedo surfaces can be captured with MESMA models. . Relative high mapping accuracies were achieved for vegetations and impervious surfaces. R^2 and RMSE of vegetation fraction are 0.79 and 7.1%, respectively (Figure 3, 4, 5, 6). The estimation of impervious surfaces obtained similar accuracy, with R^2 0.72 and RMSE 10.7%. Both mean and HSDC normalized models made a notable improvement in mapping vegetation fraction and slight improvement in mapping impervious surface fractions, comparing with the standard SMA (Figure 7, 8, 9, 10). Both two normalizations can only suppress spectral variation with similar spectral shape. HSDC is slightly better than mean normalization in reducing the effects of illumination and spectral variability of urban land surface.

REFERENCES

Adams, J. B.,1986. Spectral mixture modeling: A new analysis of rock and soil types at the Viking Lander1 site. *Journal of Geophysical Research*, 91, 8089-8122.

Adams, J. B., Sabol, D. E., Kapos, V., Filho, R. A., Robert, D. A., Smith, M. O., and Gillespie, A. R.,1995. Classification of multispectral images based on fractions of endmembers: Application to land-cover change in the Brazilian Amazon. *Remote Sensing of Environment*, 52, 137-154.

Adams, J. B., Smith, M. O., and Gillespie, A. R.,1993. Imaging spectroscopy: Interpretation based on spectral mixture analysis. In *remote Geochemical Analysis: Elemental and Mineralogical composition 7*, (C. M. Pieters and P. Englerty, Eds.), Cambridge University Press, New York, pp. 145-166.

Boardman, J. W., Kruse, F. A., and Green, R. O.,1995, Mapping target signatures via partial unmixing of AVIRIS data: in Summaries, Fifth JPL Airborne Earth Science Workshop, JPL Publication 95-1, v. 1, p. 23-26.

Chavez, P. S.,1996. Image-based atmospheric correction: Revisited and improved. *Photogrammetric Engineering and Remote Sensing*, 62, 1025-1036.

Chuvieco, E., Riaňo, D., Aguado, I., and Cocero, D.,2002. Estimation of fuel moisture content from multitemporal analysis of Landsat Thematic Mapper reflectance data: applications in

fire danger assessment. *International Journal of Remote Sensing*, 23 (11), 2145-2162.

Green, A. A., Berman, M., Switzer, P., and Craig, M. D.,1988. A transformation for ordering multispectral data in terms of image quality with implications for noise removal. *IEEE Transactions on Geoscience and Remote Sensing*, 26, 65-74.

Markham, B. L., Boncyk, W. C., Helder, D. L., and Barker, J. L.,1997. Landsat-7 enhanced thematic mapper plus radiometric calibration. *Canadian Journal of Remote Sensing*, 23 (4), 318-332.

Pouch, G. W., & Campagna, D. J.,1990. Hyperspherical direction cosine transformation for separation of spectral and illumination information in digital scanner data. *Photogrammetric Engineering and Remote Sensing*, 56, 475-479.

Powell, R. L., Robert, D. A., Dennsion, P. E., and Hess, L. L.,2007. Sub-pixel mapping of urban land cover using multiple endmember spectral mixture analysis: Manaus, Brazil. *Remote Sensing of Environment*, 106, 253-267.

Rashed, T., Weeks, J. R., Roberts, D., Rogan, J., and Powell, R.,2003. Measuring the physical composition of urban morphology using multiple endmember spectral mixture models. *Photogrammetric Engineering and Remote Sensing*, 69, 1011-1020.
Ridd, M. K.,1995. Exploring a V-I-S (vegetation-impervious surface-soil) model for urban ecosystem analysis through remote sensing: comparatice anatomy for cities. *International Journal of Remote Sensing*, 16, 2165-1185.

Robert, D. A., Gardner, M., Church, R., Ustin, S., Scheer, G. and Green, R. O.,1998. Mapping chaparral in the Santa Monica Mountains using multiple endmember spectral mixture models. *Remote Sensing of Environment* 65: 257-279.

Small, C.,2001. Estimation of urban vegetation abundance by spectral mixture analysis. *International Journal of Remote Sensing*, 22, 1305-1334.

Small ,C.,2003. High spatial resolution spectral mixture analysis of urban reflectance. *Remote Sensing of Environment*, 88, 170-186.
Small, C.,2005. Global analysis of urban reflectance. *International Journal of Remote Sensing*, 26(4), 661-681.

Wu, C.,2004. Normalized spectral mixture analysis for monitoring urban composition using ETM+ imagery. *Remote Sensing of Environment*, 93, 480-492.

Wu, C., and Murray, A. T.,2003. Estimating impervious surface distribution by spectral mixture analysis, *Remote Sensing of Environment*, 84, 493-505.